JACS
JOURNAL OF THE AMERICAN CHEMICAL SOCIETY

Communication

pubs.acs.org/JACS

Soluble Precursors for $CuInSe_2$, $CuIn_{1-x}Ga_xSe_2$, and $Cu_2ZnSn(S,Se)_4$ Based on Colloidal Nanocrystals and Molecular Metal Chalcogenide Surface Ligands

Chengyang Jiang,[†] Jong-Soo Lee,[†] and Dmitri V. Talapin*[,†,‡]

[†]Department of Chemistry and James Frank Institute, University of Chicago, Chicago, Illinois 60637, United States

[‡]Center for Nanoscale Materials, Argonne National Laboratory, Argonne, Illinois 60439, United States

Supporting Information

ABSTRACT: We report a new platform for design of soluble precursors for $CuInSe_2$ (CIS), $Cu(In_{1-x}Ga_x)Se_2$ (CIGS), and $Cu_2ZnSn(S,Se)_4$ (CZTS) phases for thin-film potovoltaics. To form these complex phases, we used colloidal nanocrystals (NCs) with metal chalcogenide complexes (MCCs) as surface ligands. The MCC ligands both provided colloidal stability and represented essential components of target phase. To obtain soluble precursors for $CuInSe_2$, we used $Cu_{2-x}Se$ NCs capped with $In_2Se_4^{2-}$ MCC surface ligands or $CuInSe_2$ NCs capped with $\{In_2Cu_2Se_4S_3\}^{3-}$ MCCs. A mixture of $Cu_{2-x}Se$ and ZnS NCs, both capped with $Sn_2S_6^{4-}$ or $Sn_2Se_6^{4-}$ ligands was used for solution deposition of CZTS films. Upon thermal annealing, the inorganic ligands reacted with NC cores forming well-crystallized pure ternary and quaternary phases. Solution-processed CIS and CZTS films featured large grain size and high phase purity, confirming the prospects of this approach for practical applications.

Traditional semiconductor technologies cannot be directly used for large area photovoltaic (PV) applications because of cost limitations. As a lower cost alternative, spin coating, spray-coating, dip coating, or inkjet printing could enable inexpensive roll-to-roll device fabrication. In recent years, liquid-phase deposition of inorganic semiconductors has attracted much attention,[1] with special interest paid to the materials suitable for efficient thin-film PV devices. Among these, $CuInSe_2$ (CIS) and $Cu(In,Ga)Se_2$ (CIGS) demonstrated best PV performance[2] due to their optimal band-gaps, high absorption coefficients, and high photostability associated with "self-healing" mechanisms.[3] Another exciting material is $Cu_2ZnSn(S,Se)_4$ (CZTS) which includes only earth-abundant nontoxic elements.[4,5] In 2010, Todorov et al. demonstrated CZTS-based solar cells with energy conversion efficiency 9.6%.[6]

Several families of soluble molecular precursors for CIS and CIGS have been explored during last decades. Among them are the organometallic compounds[7] and hydrazinium chalcogenidometallates.[8−10] These molecular precursors contain sacrificial groups that chemically bind to metal or chalcogen ions to provide solubility in a desired solvent. Elimination of these sacrificial groups during thermal decomposition of the precursor into an inorganic phase usually results in substantial volume contraction, generating cracks and discontinuities in obtained inorganic materials. To generate high quality semiconductor layers, the precursor should not contain any bulky sacrificial ligands while maximizing the ratio between the number of deposited atoms (i.e., metals and chalcogens) and the total number of atoms in soluble precursor. As an example, Mitzi's discovery of soluble hydrazinium chalcogenidometallates led to a breakthrough in soluble molecular precursors for thin semiconducting films[8,11,12] because small sacrificial groups ($N_2H_5^+$, N_2H_4, and chalcogenide ions) allowed for high atom economy during the precursor-to-semiconductor transformation. The weight losses associated with the transformation process were in the range of 25% (for CIS)[8] to 35% (for SnS_2).[11] We are aware of only one report on CZTS deposited from the molecular precursors.[13] As the close analogue, Todorov et al. combined the hydrazinium molecular precursors for Cu_2S and $SnSe_2$ with microscopic ZnSe particles in form of a hydrazine-based slurry that converted into copper-deficient CZTS phase upon annealing at 540 °C.[6]

Switching from molecular precursors that contain only one or few metal atoms to larger soluble species like clusters or nanocrystals (NCs) can allow for further improvements of the atom economy during the precursor-to-semiconductor transformation. For example, CIS,[14] CIGS,[15] and CZTS[16−18] NCs were used as soluble precursors for semiconducting films. This approach requires NC sintering or establishing good electronic connectivity between individual NCs. The major obstacle here is that colloidal NCs are typically stabilized by organic surface ligands that form insulating barriers between the NCs. These surface ligands also often inhibit the formation of large crystalline grains upon NC sintering and leave behind undesirable carbonaceous impurities.[19] Here, we show that attaching molecular metal chalcogenide complexes, MCC's,[20] to the NC surface introduces a platform for design of chemical transformations leading to pure ternary and quaternary CIS, CIGS, and CZTS phases. The conversion of soluble NC−MCC precursors into dense semiconductor film can occur with weight losses as small as 2−3% that prevent cracking and void formation. Moreover, in many cases, this chemistry does not require hydrazine as a reactant or solvent, thus, providing a convenient route to environmentally benign and scalable manufacturing of solution-processed PV materials.

Received: November 10, 2011
Published: February 13, 2012

dx.doi.org/10.1021/ja2105812 | J. Am. Chem. Soc. 2012, 134, 5010−5013

Several combinations of NCs and MCC ligands can serve as soluble precursors for CIS. We used $Cu_{2-x}Se$ NCs (x = 0−0.2) with $In_2Se_4^{2-}$ surface ligands bound to the NC surface and $N_2H_5^+$ as sacrificial counterions (Figure 1A).[20,21] First, we

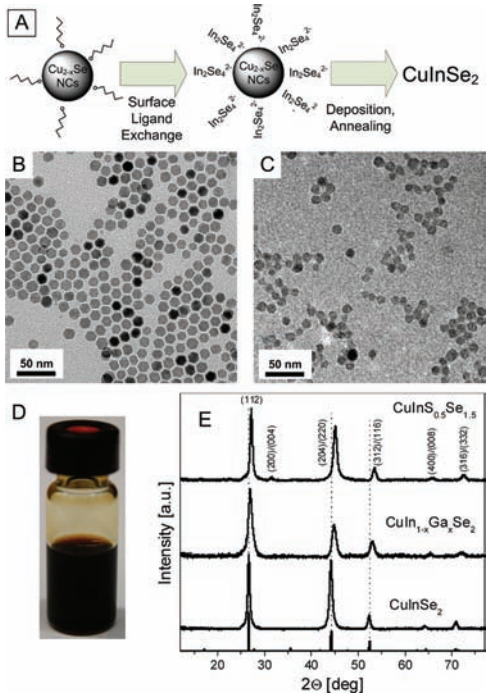

Figure 1. (A) Typical synthetic route. (B) TEM image of as-synthesized, oleylamine capped $Cu_{2-x}Se$ NCs. (C) TEM image of In_2Se_3-MCCs capped $Cu_{2-x}Se$ NCs. (D) Photograph of $Cu_{2-x}Se$ NCs capped with $In_2Se_4^{2-}$ MCCs. (E) XRD patterns of annealed $CuInSe_2$, $CuIn_{1-x}G_xSe_2$ and $CuInS_{0.5}Se_{1.5}$ thin films. The X-ray reflections from bulk $CuInSe_2$ are shown as the line patterns.

synthesized monodisperse, cubic-phase $Cu_{2-x}Se$ NCs capped with oleylamine (Figures 1B and S1A,B).[31,23] To introduce indium, oleylamine ligands were exchanged with $In_2Se_4^{2-}$ MCCs. The ligand exchange accompanied with the phase transfer of $Cu_{2-x}Se$ NCs from nonpolar hexane phase into a polar solvent (mixture of dimethylsulfoxide (DMSO) and ethanolamine (EA), 5:3 v/v) containing dissolved $In_2Se_4^{2-}$ species. The complete removal of original hydrocarbon ligands has been also confirmed in FTIR studies (Figure S1C). The negative charge on the MCC ligands (estimated average ζ-potential −31 mV, Figure S1D) provided electrostatic stabilization for colloidal solutions of MCC-capped NCs in polar solvents.[20] The TEM image (Figure 1C) showed that the morphology of $Cu_{2-x}Se$ NCs was preserved after the ligand exchange. The XRD pattern (Figure S1A) further confirmed the presence of original cubic phase of $Cu_{2-x}Se$ NCs. $Cu_{2-x}Se$ NCs and equivalent molar amount of $In_2Se_4^{2-}$ MCCs formed stable colloidal solutions in DMSO/EA mixture (Figure 1D). These NCs can be separated by the addition of acetonitrile and subsequent centrifugation. Precipitated $Cu_{2-x}Se$ NCs were redispersed in a small amount of various polar solvents (DMSO and EA; *N*,*N*-dimethylformamide (DMF); and *N*,*N*-dimethylacetamide (DMA)) in the presence of free $In_2Se_4^{2-}$ MCC, forming a concentrated colloidal solution, suitable for deposition of CIS films by spin- or spray coating. After annealing at 500 °C, the films of $Cu_{2-x}Se$ NCs capped with $In_2Se_4^{2-}$ MCCs transformed into pure CIS phase, as evidenced by XRD patterns (Figure 1E and S2).[22] Partial replacement of $In_2Se_4^{2-}$ with equivalent amount of gallium selenide MCC[20] resulted in the formation of quaternary $CuIn_{1-x}Ga_xSe_2$ (CIGS) phase known as excellent PV material.[31] Cu_2S NCs can also be used in this system as a substitution for $Cu_{2-x}Se$ NCs, leading to $CuInS_{0.5}Se_{1.5}$ thin films (Figure 1E). The copper/indium, indium/gallium, and sulfur/selenium ratios can be fine-tuned by adjusting the amounts of NCs and MCCs. The latter can be present in solution both as the surface ligands adhered to the NC surface and as free molecular species. We used ICP-OES measurements of the molecular precursor composition for fine-tuning CIS and CIGS stoichiometry. The use of NC−MCC precursors allowed formation of CIS and CIGS phases using relatively benign solvents. We found $In_2Se_4^{2-}$ and gallium selenide MCCs are stable and soluble in different polar solvents (formamide (FA), DMF, DMA, DMSO and EA, etc.), whereas $Cu_7S_4^-$ species used as the copper source by Mitzi et al.[8] form stable solutions only in hydrazine. Switching to $Cu_{2-x}Se$ NCs significantly expands the list of solvents suitable for solution-based processing of CIS and CIGS.

The solid-state reaction between $Cu_{2-x}Se$ NCs and $In_2Se_4^{2-}$ MCCs takes place upon heat treatment. Simple calculations based on the 1:1 molar ratio between copper and indium predict that the transformation of $Cu_{2-x}Se$ NCs capped with $In_2Se_4^{2-}$ MCCs (Figure S1F) into CIS phase should occur with 20.6% weight loss. The experimental TGA measurements showed 20.9% weight loss (Figure 2A), in very good agreement

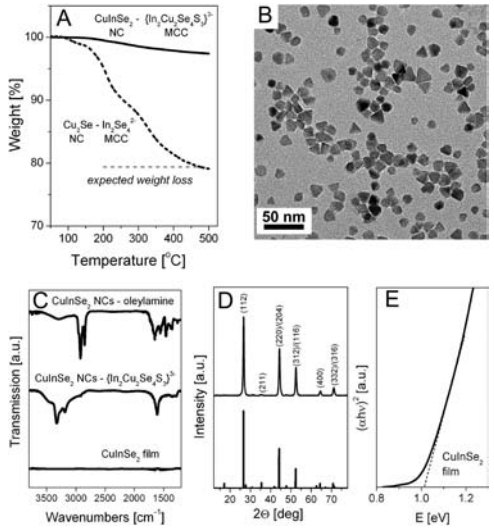

Figure 2. (A) TGA scans for $CuInSe_2$ NCs capped with $CuInSe_2$-MCCs dried from N_2H_4 (solid line) and for $Cu_{2-x}Se$ NCs capped with $In_2Se_4^{2-}$ MCCs dried from the mixture of DMSO and EA (dash line). (B) TEM image of $CuInSe_2$ NCs capped with $CuInSe_2$-MCCs. (C) FTIR spectra of $CuInSe_2$ NCs at different stages of the transformation. (D) XRD pattern of annealed CIS thin film (JCPDS #40-1487). (E) Extrapolations of $(\alpha h\nu)^2$−E plots derived from absorption spectra of CIS thin films, showing the estimated bandgap of 1.0 eV.

with calculated value. Meanwhile the width of the X-ray peaks in Figure 1E exceeded the instrumental broadening (Figure S3) suggesting small crystal domains. We further optimized NC−MCC precursors to improve CIS grain size.

The "atom economy" during the transformation of soluble precursor to CIS or CIGS phase can be dramatically improved by using $CuInSe_2$ NCs[24] capped with the MCC ligands with nominal composition $\{In_2Cu_2Se_4S_3\}^{3-}$. Milliron et al. showed

dx.doi.org/10.1021/ja2105812 | J. Am. Chem. Soc. 2012, 134, 5010−5013

that these molecular species form pure CIS phase after annealing at 350 °C with the weight loss of 24.9%.[8] A small amount of $\{In_2Cu_2Se_4S_3\}^{3-}$, about 0.1 mol equiv, was sufficient to displace original oleylamine capping ligands and stabilize colloidal solutions of ~16 nm $CuInSe_2$ NCs. TEM images (Figures 2B and S5A) and XRD patterns (Figure S5B) confirmed that $CuInSe_2$ NCs remained intact after the ligand exchange. Meanwhile, FTIR spectra (Figure 2C) showed complete removal of organic surfactants since the strong peaks at 3000−2800 cm^{-1} indicating C−H vibrations were replaced by broad peaks at 3500−3000 cm^{-1} corresponding to N−H vibrations from N_2H_4 and $N_2H_5^+$ ions. As the decomposition of MCCs was the only source of the weight loss upon annealing, the formation of a continuous crystalline CIS phase from the soluble precursor occurred with only 2.6% weight loss (Figure 2A,D). The width of the X-ray diffraction peaks was determinded by the instrumental broadening (Figure S3).[31] Concentrated NC−MCC solutions formed uniform, continuous CIS films with large grains (Figure S4A,B) suggesting that small weight loss and associated volume contraction determine the continuity of obtained semiconductor. The absorption measurements were conducted for CIS thin films prepared by spin-coating colloidal solutions of $CuInSe_2$ NCs capped with $\{In_2Cu_2Se_4S_3\}^{3-}$ MCCs. The extrapolation of $(\alpha h\nu)^2$−E plots to the x-axis showed that the bandgap of the material was 1.01 eV (Figure 2E), in a very good agreement with the bandgap of bulk $CuInSe_2$.[2]

Small amount of $In_2Se_4^{2-}$ MCC ligands also provide colloidal stability to $CuInSe_2$ NCs. As discussed, using $In_2Se_4^{2-}$ in lieu of $\{In_2Cu_2Se_4S_3\}^{3-}$ significantly expands the list of available solvents.[22] The TEM image (Figure S6A) has proven the preservation of $CuInSe_2$ NCs in this scenario, while the XRD pattern (Figure S6B) showed pure CIS phase after annealing. Moreover, the capping of $CuInSe_2$ NC surface with Ga_2Se_3-MCCs[20] allowed us to fabricate Cu-deficient CIGS with minimal weight losses during solid-state transformation of soluble precursor into a continuous phase (Figure S6B,C).

To prepare soluble precursors for solution deposition of CZTS films, we started with colloidal $Cu_{2-x}Se$ NCs and ZnS NCs,[25,26] both capped with long-chain alkylamine ligands, and treated them with well-characterized and robust $(NH_4)_4Sn_2S_6$ MCCs.[27] Both NCs easily exchanged original capping ligands for $Sn_2S_6^{4-}$ ions and formed stable colloidal solutions in FA (Figure 3A) or *N*-methylformamide (MF). In both cases, we used 0.5 mol equiv of $(NH_4)_4Sn_2S_6$ (with respect to NCs). The compositional fine-tuning could be easily achieved by adjusting the amount of $(NH_4)_4Sn_2S_6$ added to NCs. To prepare completely transparent, colorless, and stable colloidal solutions of $Sn_2S_6^{4-}$ capped ZnS NCs in FA, it was helpful to purge an excess of NH_3 through the solution. TEM images showed very similar $Cu_{2-x}Se$ and ZnS particles compared to the original NCs capped with organic ligands (Figures S7A,B, S8A, 1B). XRD patterns of ZnS NCs (Figures 3B,S8B) and $Cu_{2-x}Se$ NCs (Figure 3B, S1A) confirmed that NCs retained their original structures during the ligand exchange. The dynamic light scattering measurements (Figure S7C,D) demonstrated that both $Cu_{2-x}Se$ and ZnS colloidal solutions in FA contained negatively charged, monodisperse, and aggregate-free nanoparticles, while FTIR spectra (Figure S9) proved that the organic ligands on both NCs were completely replaced with $Sn_2S_6^{4-}$ MCCs. To further purify and concentrate the colloidal solutions, both $Sn_2S_6^{4-}$-capped $Cu_{2-x}Se$ NCs and $Sn_2S_6^{4-}$-capped ZnS NCs were precipitated from FA with acetonitrile

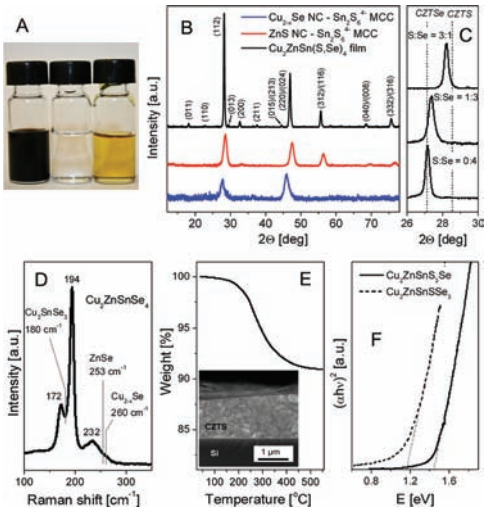

Figure 3. (A) Photograph of colloidal solutions of $Cu_{2-x}Se$ NCs (left), ZnS NCs (middle), and ZnSe NCs (right), all capped with $Sn_2S_6^{4-}$ MCC ligands. (B) XRD patterns of $Sn_2S_6^{4-}$ capped $Cu_{2-x}Se$ NCs, $Sn_2S_6^{4-}$ capped ZnS NCs, and $Cu_2ZnSn(S,Se)_4$ (CZTS) thin film. (C) XRD patterns of CZTS thin films with different S/Se ratios. Vertical lines indicate the position of 112 reflections in bulk $Cu_2ZnSnSe_4$ (left line) and Cu_2ZnSnS_4 phases (right line). (D) Raman spectrum of $Cu_2ZnSnSe_4$ film also showing the Raman shifts for typical impurity phases. (E) TGA scan for NC−MCC mixture targeting CZTS (inset: cross-sectional SEM of CZTS thin film). (F) Extrapolations of $(\alpha h\nu)^2$−E plots derived from the absorption spectra of $Cu_2ZnSnSSe_3$ (dashed line) and Cu_2ZnSnS_3Se (solid line) thin films, showing the estimated bandgaps of 1.16 and 1.44 eV, respectively.

and then redispersed in a small volume of FA or MF with appropriate amount of free $Sn_2S_6^{4-}$ ligands estimated from ICP-OES measurements for Cu, Zn, and Sn. MCC-capped smaller NCs typically showed higher solubility in FA. For instance, when 4 nm ZnS NCs or 5 nm ZnSe NCs[28](Figure S8C,D) were used instead of 9 nm ZnS NCs, colloidal solutions with concentration over 50 mg/mL were readily obtained.

The solutions containing equal molar amounts of $Sn_2S_6^{4-}$-capped $Cu_{2-x}Se$ NCs and $Sn_2S_6^{4-}$-capped ZnS NCs were combined together without any losses of colloidal stability, deposited and annealed at 500 °C in inert atmosphere. Annealing for 20 min was sufficient to obtain highly crystalline CZTS films (Figure S2).[31] The XRD patterns of obtained films (Figure 3B) can be assigned to well-crystallized $Cu_2ZnSn(S,Se)_4$ kesterite phase showing all weak diffraction peaks characteristic of kesterite phase (Figure S10A). All diffraction peaks were shifted to smaller angles by ~0.3 degree with respect to Cu_2ZnSnS_4 X-ray pattern (JCPDS#26-0575) because of partial substitution of S atoms with Se atoms which caused increase of the lattice constant by 1.1%. To further demonstrate the possibility of compositional tuning of CZTS films, we used several combinations of NCs and MCCs targeting different CZTS compositions. First, 5.2 nm ZnSe NCs were combined with 14 nm $Cu_{2-x}Se$ NCs, both capped with $Sn_2Se_6^{4-}$.[31] This formulation resulted in pure $Cu_2SnZnSe_4$ phase (Figure 3C). CZTS phase with S/Se ratio of 1:3 was prepared by combining Cu_2Se NCs capped with $Sn_2S_6^{4-}$ MCCs and ZnSe NCs, capped with $Sn_2Se_6^{4-}$ MCCs. These NCs demonstrated excellent solubility in FA and resulted in thin films whose XRD patterns matched those expected for $Cu_2ZnSnSSe_3$ (Figure 3C).

Raman spectroscopy further confirmed the formation of pure kesterite phase during the solid-state transformation MCC-

dx.doi.org/10.1021/ja2105812 | J. Am. Chem. Soc. 2012, 134, 5010−5013

capped NCs (Figures 3D and S11). The Raman spectra for $Cu_2SnZnSe_4$ and Cu_2SnZnS_3Se perfectly matched the literature data for respective phases[31,29,30] and showed no unreacted precursors or impurity phases. Figure S12 shows Raman microscopy mapping of CZTS film surface that confirmed homogeneity film and phase purity over macroscopic areas. The annealing temperature played in important role for purity of CZTS phase. For example the annealing at 600 °C for 1 h resulted in a partial transformation of CZTS phase into $Cu_2Sn(S,Se)_3$ (Figure S10B). TGA data indicated that the system underwent only 9.1% weight loss during annealing (Figure 3E), in good agreement with the calculated value 10.3%. We found that pure CZTS phase formed at 350−400 °C, whereas annealing at 500 °C resulted in a significant increase of the grain size confirmed by narrowing of X-ray diffraction peaks (Figure S10B). Cross-sectional SEM image (inset in Figure 3E and Figure S4C,D) showed that individual $Sn_2S_6^{4-}$ capped $Cu_{2-x}Se$ and ZnS NCs converted into large and densely packed CZTS grains. We hypothesize that efficient transformation of NCs into a uniform CZTS phase is facilitated by a good match between the NC size and the characteristic width of the reaction zone for solid-state reactions.[31]

The extrapolation of $(\alpha h\nu)^2-h\nu$ plots obtained from the absorption spectra of spin-coated thin films (Figure 3F) showed 1.44 eV bandgap, between 1.5 eV reported for pure sulfide CZTS, and 1.0 eV reported for pure selenide CZTSe.[32] This band gap value is in agreement with XRD and ICP-OES data showing S/Se ∼ 3:1. As expected, the decrease of S/Se ratio resulted in the red shift of the absorption edge due to a decrease of E_g down to 1.16 eV for S/Se ∼ 1:3 ratio. Our preliminary charge transport studies revealed p-type conductivity in both CIS and CZTS films. Figure S13 shows field-effect transistor (FET) measurements for spray coated CZTS film annealed at 500 °C for 1 h. The drain current increased with applying negative voltage to the gate electrode that is typical for p-type transport. The hole mobility corresponding to the linear regime of FET operation measured at V_{DS} = −5 V was μ_{lin} = 0.79 $cm^2\ V^{-1}\ s^{-1}$, in the range desirable for PV applications.

In summary, $CuInSe_2$, $CuIn_{1-x}Ga_xSe_2$, and $Cu_2ZnSn(S,Se)_4$ thin films have been synthesized using a novel class of soluble precursors combining colloidal NCs and molecular metal chalcogenide ligands. These precursors can be readily transformed into continuous films of PV relevant semiconductors in a very atom-economic way, with minimal weight loss and volume contraction. Described methodology can be applied to design of soluble precursors for different inorganic phases.

■ ASSOCIATED CONTENT

Supporting Information

Additional experimental details and Figures. This material is available free of charge via the Internet at http://pubs.acs.org.

■ AUTHOR INFORMATION

Corresponding Author

dvtalapin@uchicago.edu

Notes

The authors declare no competing financial interest.

■ ACKNOWLEDGMENTS

We thank M. V. Kovalenko for synthesis of SnS_2. This work was supported by NSF CAREER under Award Number DMR-0847535 and DOE SunShot Program. We acknowledge infrastructure support by the NSF MRSEC Program under Award Number DMR-0213745. The use of the Center for Nanoscale Materials was supported by the U.S. Department of Energy, Office of Science, Office of Basic Energy Sciences, under Contract No. DE-AC02-06CH11357.

■ REFERENCES

(1) Todorov, T.; Mitzi, D. B. *Eur. J. Inorg. Chem.* **2010**, 17.
(2) Stanberry, B. J. *Crit. Rev. Solid State Mater. Sci.* **2002**, *27*, 73.
(3) Guillemoles, J.-F.; Rau, U.; Kronik, L.; Schock, H.-W.; Cahen, D. *Adv. Mater.* **1999**, *11*, 957.
(4) Katagiri, H. *Thin Solid Films* **2005**, *480−481*, 426.
(5) Katagiri, H.; Jimbo, K.; Maw, W. S.; Oishi, K.; Yamazaki, M.; Araki, H.; Takeuchi, A. *Thin Solid Films* **2009**, *517*, 2455.
(6) Todorov, T. K.; Reuter, K. B.; Mitzi, D. B. *Adv. Mater.* **2010**, *22*, E156−E159.
(7) Castro, S. L.; Bailey, S. G.; Raffaelle, R. P.; Banger, K. K.; Hepp, A. F. *Chem. Mater.* **2003**, *15*, 3142.
(8) Milliron, D. J.; Mitzi, D. B.; Copel, M.; Murray, C. E. *Chem. Mater.* **2006**, *18*, 587.
(9) Mitzi, D. B.; Yuan, M.; Liu, W.; Kellock, A., J.; Chey, S. J.; Deline, V.; Schrott, A. G. *Adv. Mater.* **2008**, *20*, 3657.
(10) Liu, W.; Mitzi, D. B.; Yuan, M.; Kellock, A., J.; Chey, S. J.; Gunawan, O. *Chem. Mater.* **2010**, *22*, 1010.
(11) Mitzi, D. B.; Kosbar, L. L.; Murray, C. E.; Copel, M.; Afzali, A. *Nature* **2004**, *428*, 299.
(12) Mitzi, D. B.; Copel, M.; Chey, S. J. *Adv. Mater.* **2005**, *17*, 1285.
(13) Ki, W.; Hillhouse, H. W. *Adv. Energy Mater.* **2011**, *1*, 732.
(14) Guo, Q.; Kim, S. J.; Kar, M.; Shafarman, W., N.; Birkmire, R. W.; Stach, E. A.; Agrawal, R.; Hillhouse, H. W. *Nano Lett.* **2008**, *8*, 2982.
(15) Panthani, M. G.; Akhavan, V.; Goodfellow, B.; Schmidtke, J. P.; Dunn, L.; Dodabalapur, A.; Barbara, P. F.; Korgel, B. A. *J. Am. Chem. Soc.* **2008**, *130*, 16770.
(16) Riha, S. C.; Parkinson, B. A.; Prieto, A. L. *J. Am. Chem. Soc.* **2009**, *131*, 12054.
(17) Guo, Q.; Hillhouse, H. W.; Agrawal, R. *J. Am. Chem. Soc.* **2009**, *131*, 11672.
(18) Steinhagen, C.; Panthani, M. G.; Akhavan, V.; Goodfellow, B.; Koo, B.; Korgel, B. A. *J. Am. Chem. Soc.* **2009**, *131*, 12554.
(19) Ridley, B. A.; Nivi, B.; Jacobson, J. M. *Science* **1999**, *286*, 746.
(20) Kovalenko, M. V.; Scheele, M.; Talapin, D. V. *Science* **2009**, *324*, 1417.
(21) Lee, J.-S.; Kovalenko, M. V.; Huang, J.; Chung, D. S.; Talapin, D. V. *Nat. Nano* **2011**, *6*, 348.
(22) Additional details provided in Supporting Information.
(23) Dorfs, D.; Hartling, T.; Miszta, K.; Bigall, N. C.; Kim, M. R.; Genovese, A.; Falqui, A.; Povia, M.; Manna, L. *J. Am. Chem. Soc.* **2011**, *133*, 11175.
(24) Tang, J.; Hinds, S.; Kelley, S. O.; Sargent, E. H. *Chem. Mater.* **2008**, *20*, 6906.
(25) Joo, J.; Na, H. B.; Yu, T.; Yu, J. H.; Kim, Y. W.; Wu, F.; Zhang, J. Z.; Hyeon, T. *J. Am. Chem. Soc.* **2003**, *125*, 11100.
(26) Yu, J. H.; Joo, J.; Park, H. M.; Baik, S.-I.; Kim, Y. W.; Kim, S. C.; Hyeon, T. *J. Am. Chem. Soc.* **2005**, *127*, 5662.
(27) Kovalenko, M. V.; Bodnarchuk, M., I.; Zaumseil, J.; Lee, J.-S.; Talapin, D. V. *J. Am. Chem. Soc.* **2010**, *132*, 10085.
(28) Cozzoli, P. D.; Manna, L.; Curri, M. L.; Kudera, S.; Giannini, C.; Striccoli, M.; Agostiano, A. *Chem. Mater.* **2005**, *17*, 1296.
(29) Altosaar, M.; Raudoja, J.; Timmo, K.; Danilson, M.; Grossberg, M.; Krustok, J.; Mellikov, E. *Phys. Status Solidi A* **2008**, *205*, 167.
(30) Mitzi, D. B.; Gunawan, O.; Todorov, T. K.; Wang, K.; Guha, S. *Sol. Energy Mater. Sol. Cells* **2011**, *95*, 1421.
(31) Son, D. H.; Hughes, S. M.; Yin, Y.; Paul Alivisatos, A. *Science* **2004**, *306*, 1009.
(32) Chen, S.; Gong, X. G.; Walsh, A.; Wei, S.-H. *Appl. Phys. Lett.* **2009**, *94*, 041903.